

Asymmetric Dark Matter and Sommerfeld Enhancement

Sujuan Qiu, Hoernisa Iminniyaz*, Wensheng Huo

*School of Physics Science and Technology, Xinjiang University,
Urumqi 830017, China*

Abstract

We show that the relic density of asymmetric dark matter with long-range interactions is affected by the Sommerfeld enhancement. The annihilation cross section of asymmetric dark matter is enhanced due to the Sommerfeld effect. It results the relic density is decreased. Using the Planck data, the constraints on the asymmetry factor and coupling required to attain the observed dark matter density are obtained. We derive the upper bounds on the mass for asymmetric dark matter in s -wave and p -wave annihilation cases.

arXiv:2403.01682v1 [hep-ph] 4 Mar 2024

*Corresponding author, wrns@xju.edu.cn

1 Introduction

Recently a number of models of asymmetric Dark Matter (DM) are proposed as an alternative of symmetric DM for which the particle and antiparticle are identical [1, 2, 3]. Asymmetric DM models offer an effective explanation for the similarity of DM and baryon abundances, $\Omega_{DM} \sim \Omega_b$ [4]. In asymmetric DM scenarios, DM is not neutral, and self-conjugate, rather DM possesses particle-antiparticle asymmetry. In that case, the final abundance is determined not only by the annihilation cross section, but also by the asymmetry factor which is the difference between the particle and antiparticle abundances [5, 6]. The antiparticle abundance is largely depressed to the negligible levels when the thermal bath temperature is much lower than the DM mass. The DM abundances in the presence of a particle-antiparticle asymmetry is computed in detail in Refs.[5, 6].

In asymmetric DM models, asymmetric DM is assumed to couple to the light scalar or vector mediators [3, 7, 8, 9, 10]. The interaction between the asymmetric DM particles and antiparticles is appeared as long-range if the mediator is light enough. The wavefunction of DM particle and antiparticle is distorted by the long-range interaction. It is indeed the Sommerfeld effect [11], which leads the enhancement of DM annihilation rate at low velocities [12, 13]. The couplings required to obtain the observed DM density through the thermal freeze out mechanism of DM is suppressed due to the Sommerfeld effect [13, 14]. On the other hand, the late-time DM annihilation signals are enhanced for the certain set of couplings [15, 16, 17, 18, 19, 20, 21, 22]. Because the Sommerfeld enhancement relies on the coupling of DM to the light force mediator, for the same mass, asymmetric DM needs stronger couplings than symmetric DM, there maybe rather significant effect than symmetric DM in phenomenologically.

In Refs.[23, 24], the authors explored the effect of Sommerfeld enhancement on the relic density of asymmetric DM in detail when the light mediator is massless. The authors deduced constraints on the mass and couplings required to obtain the observed value of DM abundance in Ref.[23]. Ref.[25] discussed the impact of Sommerfeld enhancement on relic density in the case of s-wave annihilation when the mediator mass $m_\varphi \neq 0$ in model independent way. They concluded that the abundance of asymmetric DM is decreased due to the enhancement of the annihilation cross section. In the present work, we consider two minimal cases, in that scenarios, asymmetric DM is coupled to a light vector boson or a light scalar boson. We investigate the affect of Sommerfeld enhancement on the relic density of asymmetric DM for s -wave and p -wave annihilations in detail when the mediator mass $m_\varphi \neq 0$, especially the effect of p -wave Sommerfeld enhancement on the freeze out of asymmetric DM. We extend our previous analysics in several ways. First, we plot the ratio of asymmetric DM antiparticle to particle abundances with Sommerfeld enhancement as a function of the inverse-scaled tem-

perature. We find the antiparticle abundance is depleted faster while the annihilation cross section is enhanced by the Sommerfeld effect. The decrease of the ratio is significant for the larger couplings. We calculate the couplings required to attain the observed DM relic density as a function of the asymmetry factor. The coupling is larger for asymmetric case than the symmetric one with the Sommerfeld enhancement. The final abundance is largely determined by the asymmetry. When the asymmetry is large, the required mass bound is smaller. We also noticed that the maximum value of mass needed to satisfy the observed value of DM abundance is smaller than the symmetric DM. In our work, we ignored the effect of bound state formation on the relic density of asymmetric DM which affects the relic density of DM only around the unitarity bound [10, 14].

The paper is arranged as following. In section 2, we discuss the impact of Sommerfeld effect on the relic abundance of asymmetric DM for s -wave and p -wave annihilation when the mediator mass $m_\varphi \neq 0$. In section 3, we find constraints on the parameter spaces as couplings, mass and asymmetry when the annihilation cross section of asymmetric DM is modified by the Sommerfeld enhancement. The conclusion and summaries are in the last section.

2 Relic abundance of asymmetric DM including Sommerfeld enhancement

We discuss the effect of Sommerfeld enhancement on the relic density of asymmetric DM in this section. The number density of asymmetric DM particle χ (antiparticle $\bar{\chi}$) is evolved according to the following Boltzmann equation,

$$\frac{dn_{\chi(\bar{\chi})}}{dt} + 3Hn_{\chi(\bar{\chi})} = -\langle\sigma v\rangle(n_{\chi}n_{\bar{\chi}} - n_{\chi,\text{eq}}n_{\bar{\chi},\text{eq}}), \quad (1)$$

where $H = \pi T^2/M_{\text{Pl}}\sqrt{g_*/90}$ is the expansion rate in the radiation dominated era, here $M_{\text{Pl}} = 2.4 \times 10^{18}$ GeV is the reduced Planck mass, and g_* being the effective number of relativistic degrees of freedom. The equilibrium number densities are $n_{\chi(\bar{\chi}),\text{eq}} = g_{\chi} [mT/(2\pi)]^{3/2} e^{(-m \pm \mu_{\chi})/T}$, where g_{χ} is the number of intrinsic degrees of freedom of the particle. Here the chemical potentials $\mu_{\bar{\chi}} = -\mu_{\chi}$ when the asymmetric DM is in equilibrium state. Thermally averaged Sommerfeld enhanced annihilation cross section is

$$\langle\sigma v\rangle = a \langle S_s \rangle + b \langle v^2 S_p \rangle. \quad (2)$$

Here a is the s -wave contribution when $v \rightarrow 0$ and b is the p -wave contribution when s -wave is suppressed. The Sommerfeld enhancement factors for the massive mediator in the case of

s -wave and p -wave annihilations are given in [26, 27, 28, 29]. For s -wave annihilation,

$$S_s = \frac{2\pi\alpha}{v} \frac{\sinh\left(\frac{6mv}{\pi m_\phi}\right)}{\cosh\left(\frac{6mv}{\pi m_\phi}\right) - \cos\left(2\pi\sqrt{\frac{6\alpha m}{\pi^2 m_\phi} - \frac{9m^2 v^2}{\pi^4 m_\phi^2}}\right)}, \quad (3)$$

where v is the relative velocity of the annihilating asymmetric DM particle χ and antiparticle $\bar{\chi}$, and α is the coupling strength. For p -wave annihilation, the Sommerfeld enhancement factor is

$$S_p = \frac{(6\alpha m/(\pi^2 m_\phi) - 1)^2 + 36m^2 v^2/(\pi^4 m_\phi^2)}{1 + 36m^2 v^2/(\pi^4 m_\phi^2)} S_s. \quad (4)$$

Then

$$\langle S_s \rangle = \frac{x^{3/2}}{2\sqrt{\pi}} \int_0^\infty v^2 e^{-\frac{x}{4}v^2} S_s dv. \quad (5)$$

$$\langle v^2 S_p \rangle = \frac{x^{3/2}}{2\sqrt{\pi}} \int_0^\infty v^4 e^{-\frac{x}{4}v^2} S_p dv. \quad (6)$$

For convenience, Eq.(1) can be expressed in terms of $Y_{\chi(\bar{\chi})} = n_{\chi(\bar{\chi})}/s$, and $x = m/T$, here $s = 2\pi^2 g_{*s}/45 T^3$ is the entropy density, where g_{*s} is the effective number of entropic degrees of freedom. Then

$$\frac{dY_{\chi(\bar{\chi})}}{dx} = -\frac{\lambda\langle\sigma v\rangle}{x^2} (Y_\chi Y_{\bar{\chi}} - Y_{\chi,\text{eq}} Y_{\bar{\chi},\text{eq}}), \quad (7)$$

here the entropy conservation is used to derive Eq.(7) and $\lambda = 1.32 m M_{\text{Pl}} \sqrt{g_*}$, $g_* \simeq g_{*s}$ and $dg_{*s}/dx \simeq 0$.

The Boltzmann equation for particle (antiparticle) is rewritten as

$$\frac{dY_{\chi(\bar{\chi})}}{dx} = -\frac{\lambda\langle\sigma v\rangle}{x^2} (Y_{\chi(\bar{\chi})}^2 \mp \eta Y_{\chi(\bar{\chi})} - Y_{\text{eq}}^2), \quad (8)$$

here $Y_\chi - Y_{\bar{\chi}} = \eta$ is used which is obtained by subtracting the Boltzmann equations for χ and $\bar{\chi}$ in Eq.(7), where η is a constant and

$$Y_{\text{eq}}^2 = Y_{\chi,\text{eq}} Y_{\bar{\chi},\text{eq}} = (0.145 g_\chi / g_*)^2 x^3 e^{-2x}. \quad (9)$$

The Boltzmann equation (8) is solved following the standard picture of particle evolution scenarios. It is supposed the asymmetric DM particles and antiparticles were in thermal equilibrium with the standard model particles in the early universe. When the temperature drops as $T < m$ for $m > |\mu_\chi|$, the interaction rate Γ falls below the expansion rate H . At this freeze out point, asymmetric DM is decoupled from equilibrium state and the number densities of asymmetric DM in a co-moving space almost become constant [5, 6, 30]. Following the method which is used in [6], the final abundance for antiparticle is determined as

$$Y_{\bar{\chi}}(x_\infty) = \frac{\eta}{\exp\left[1.32 \eta m M_{\text{Pl}} \sqrt{g_*} \int_{\bar{x}_F}^\infty \langle\sigma v\rangle/x^2 dx\right] - 1}, \quad (10)$$

here

$$Y_{\bar{\chi}}(x_{\infty}) \equiv \lim_{x \rightarrow \infty} Y_{\bar{\chi}}(x). \quad (11)$$

The freeze out temperature \bar{x}_F is fixed by using the standard procedure that the freeze out occurred at the point when the deviation of the relic abundance $Y_{\bar{\chi}}(\bar{x}_F)$ and $Y_{\bar{\chi},\text{eq}}(\bar{x}_F)$ is the same order as the equilibrium value such as $Y_{\bar{\chi}}(\bar{x}_F) = (1 + \xi)Y_{\bar{\chi},\text{eq}}(\bar{x}_F)$. Here ξ is a constant and usually we take $\xi = \sqrt{2} - 1$ [30]. The relic abundance for particle is obtained by using $Y_{\chi} = Y_{\bar{\chi}} + \eta$,

$$Y_{\chi}(x_{\infty}) = \frac{\eta}{1 - \exp \left[-1.32 \eta m M_{\text{Pl}} \sqrt{g_*} \int_{x_F}^{\infty} \langle \sigma v \rangle / x^2 dx \right]}, \quad (12)$$

where x_F is the freeze out temperature for χ . Eqs.(10) and (12) are consistent with the constraint $Y_{\chi} = Y_{\bar{\chi}} + \eta$ only if $x_F = \bar{x}_F$. The total final DM relic density is

$$\Omega_{\text{DM}} h^2 = 2.76 \times 10^8 [Y_{\chi}(x_{\infty}) + Y_{\bar{\chi}}(x_{\infty})] m, \quad (13)$$

where $\Omega_{\chi} = \rho_{\chi}/\rho_c$ with $\rho_{\chi} = n_{\chi} m = s_0 Y_{\chi}$ and $\rho_c = 3H_0^2 M_{\text{Pl}}^2$, here $s_0 \simeq 2900 \text{ cm}^{-3}$ is the present entropy density, and H_0 is the Hubble constant.

Fig. 1 shows the ratio of the antiparticle abundance $Y_{\bar{\chi}}$ to particle abundance Y_{χ} as a function of the inverse-scaled temperature x for the Sommerfeld enhanced annihilation cross section. It is plotted using the numerical solutions of Eq.(8). Here panels (a) and (c) are for the s -wave annihilations, panels (b) and (d) are for p -wave annihilations. The particle and antiparticle abundances keep in the same amount before the decoupling from equilibrium state. After freeze out, the DM abundance becomes almost constant as stated previously which is shown in the figure. We find the affect of Sommerfeld enhancement is significant for the stronger coupling α and for the larger asymmetry factor η . In other words, the depletion of antiparticle abundance is faster when α is large. For p -wave annihilation, the decrease of the ratio is slower than s -wave annihilation.

3 Constraints

In this section we discuss two minimal cases in which asymmetric DM couples to a light vector or scalar boson. In the case of vector mediator, we consider the process $\chi\bar{\chi} \rightarrow 2\gamma$ which discussed in [23]. The Sommerfeld enhanced annihilation cross section times relative velocity is

$$(\sigma v)_{s\text{-wave}} = \sigma_0 S_s, \quad (14)$$

where the annihilation into two vector bosons is an s -wave process and the leading order cross section is $\sigma_0 = \pi\alpha^2/m^2$ [23].

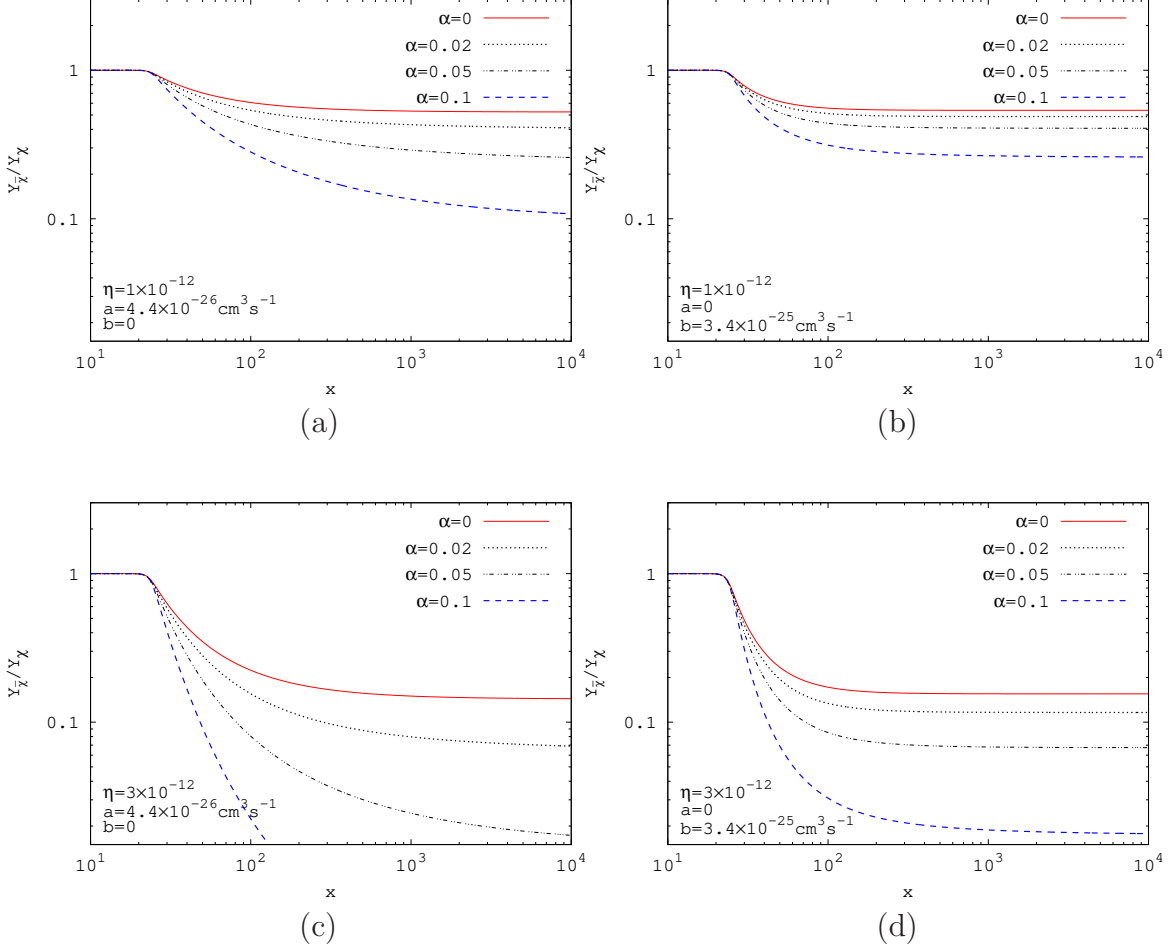


Figure 1: Ratio of asymmetric DM abundances $Y_{\bar{\chi}}$ and Y_{χ} as a function of x for the Sommerfeld enhanced annihilation cross section. Here $m = 130$ GeV, $m_{\varphi} = 0.25$ GeV, $g_{\chi} = 2$, $g_{*} = 90$.

For the scalar mediator, the process $\chi\bar{\chi} \rightarrow 2\varphi$ is considered. The annihilation cross section times relative velocity is given by

$$(\sigma v)_{p\text{-wave}} = \sigma_1 v^2 S_p, \quad (15)$$

where the annihilation of two fermions into two scalar bosons is a p -wave process and the tree level cross section is $\sigma_1 = 3\pi\alpha^2/(8m^2)$ [23].

Following we insert Eq.(14) and Eq.(15) into Eq.(8) separately and using Planck data to find constraints on the coupling strength, asymmetry factor and mass. In Fig. 2, the relation between asymmetry factor η and the coupling strength α for s -wave(p -wave) annihilation is shown for the value of total DM density $\Omega_{\text{DM}} = 0.120$ [4]. Here σ_0 and σ_1 are evaluated using the correlated α . The abundance is not sensitive for the smaller value of η . When η is small, the symmetric case is recovered. Therefore, the contour line climbs vertically (countours are independent of η). On the other hand, the smaller η gives the minimal allowed value of

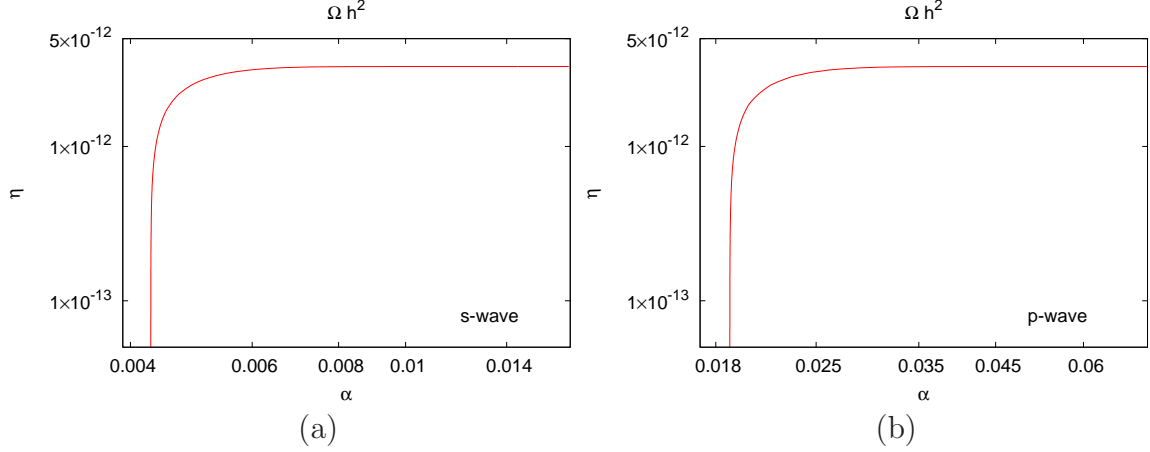


Figure 2: Contour plots of asymmetry factor η with coupling strength α for s -wave (p -wave) annihilation cross section when $\Omega_{\text{DM}}h^2 = 0.120$ [4]. Here $m = 130$ GeV, $m_\varphi = 0.25$ GeV, $g_\chi = 2$, $g_* = 90$.

the coupling strength $\alpha = 0.0043$ for s -wave and $\alpha = 0.0188$ for p -wave annihilation. The lower bound of α is larger for p -wave annihilation. The curves flatten out rapidly while the asymmetry η is increased. The relic abundance is determined by the asymmetry. In that case, the abundance is not affected when the coupling strength is increased (independent of α). A larger α , corresponds to the larger enhancement of the cross section. It leads to a smaller relic density. This should be compensated by increasing η .

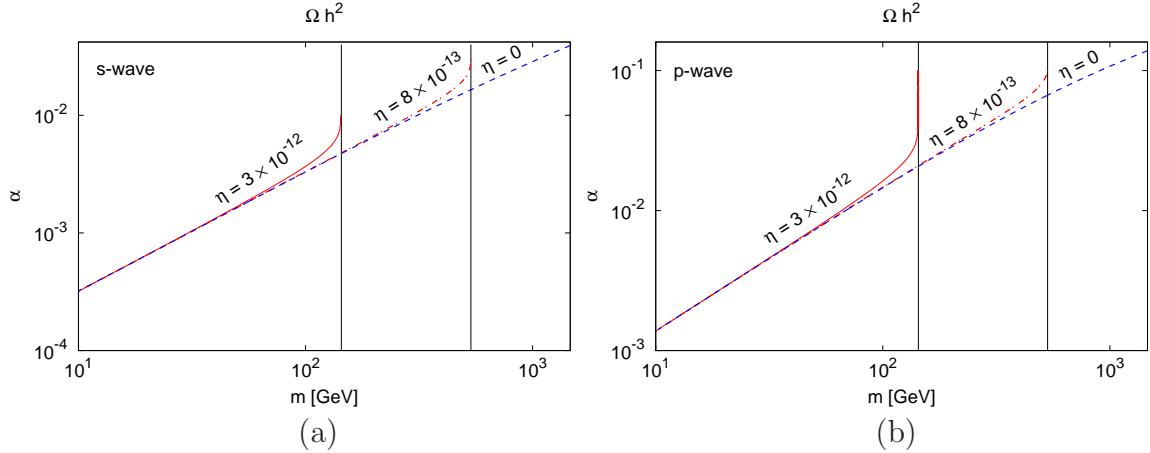


Figure 3: Contour plots of the coupling strength α and mass m for s -wave (p -wave) annihilation when $\Omega_{\text{DM}}h^2 = 0.120$ [4]. Here $m_\varphi = 0.25$ GeV, $g_\chi = 2$, $g_* = 90$, where σ_0 and σ_1 are evaluated using the correlated α .

The coupling strength required to obtain the observed value of DM relic density with mass is plotted in Fig. 3. The mass bounds for $\eta = 3 \times 10^{-12}$, 8×10^{-13} are $m = 143$, 535 GeV respectively in panel (a); $m = 143$, 532 GeV in panel (b). Highly asymmetric DM has lower

mass bound. For the same mass bound, asymmetric DM needs larger coupling to attain the observed value of DM relic density compared to the symmetric case. For example, $m = 143$, the coupling $\alpha = 0.01$ for $\eta = 3 \times 10^{-12}$ and $\alpha = 0.005$ for $\eta = 0$. The coupling for s -wave annihilation is smaller than the case of p -wave annihilation.

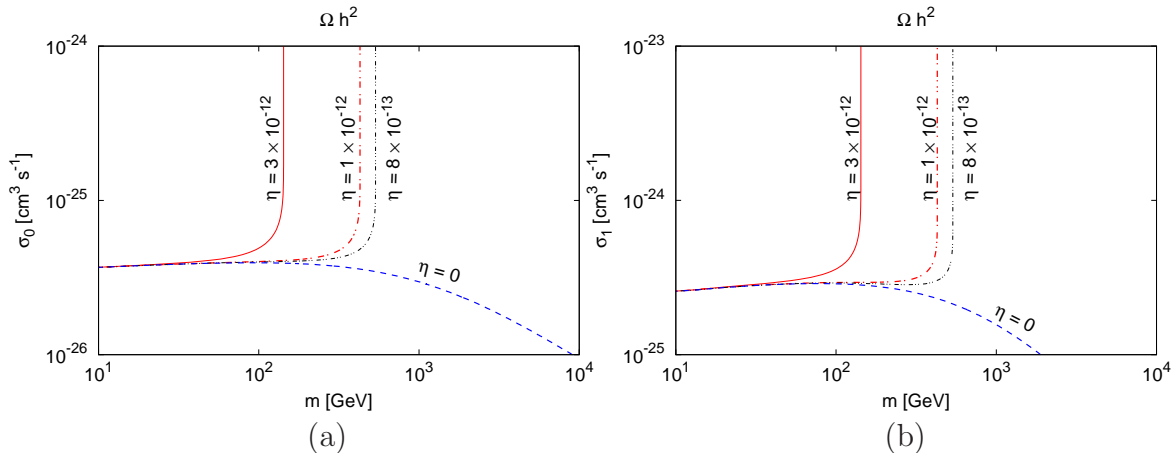


Figure 4: Contour plots of s -wave (p -wave) annihilation cross section σ_0 (σ_1) and the mass when $\Omega_{\text{DM}} h^2 = 0.120$. Here $m_\phi = 0.25$ GeV, $g_\chi = 2$, $g_* = 90$, the coupling α is computed using the expression $\sigma_0 = \pi\alpha^2/m^2$ for s -wave and $\sigma_1 = 3\pi\alpha^2/(8m^2)$ for p -wave annihilations.

The contour plots of the cross section with mass are shown in Fig. 4. The allowed region is bounded by the cross section from below and by the maximum value of m_{max} from the right for different asymmetry. For $m \ll m_{\text{max}}$, coupling constant α and σ_0 (σ_1) trace the symmetric DM ($\eta = 0$) case closely. When the cross section is small, the abundance is insensitive for the increased mass. On the other hand, while α is small, the effect of Sommerfeld enhancement is not significant for both the symmetric and asymmetric DM. When the mass reached the maximum value $m \simeq m_{\text{max}}$, the Sommerfeld enhanced annihilation cross section is increased to satisfy the observed value of the DM relic density for asymmetric DM. In the symmetric case, for larger m , the coupling is stronger (see Fig. 3), then the Sommerfeld enhanced cross section reduces the relic density notably, the cross section should be small in order to obtain the required value of the relic density. Therefore, the cross section falls quickly when the mass is increased in symmetric case.

4 Summary and conclusions

When the asymmetric DM coupled to the light force carrier, the annihilation cross section is enhanced by the Sommerfeld effect. We discuss the effect of Sommerfeld enhancement on the relic density of asymmetric DM for s -wave and p -wave annihilations for the case of light

mediator $m_\varphi \neq 0$ in detail. We found the antiparticle abundance is depleted faster than the standard case due to the Sommerfeld enhanced annihilation cross section. The decrease of the ratio of antiparticle abundance to particle abundance is larger for the stronger coupling α .

We apply our method to two kinds of scenarios, asymmetric DM coupled to either light vector mediator or the scalar mediator. We use Planck data to find constraints on the coupling constant α , asymmetry factor η and the mass value. We found when η is small, the abundance is independent of η , it is indeed the symmetric case. The minimal value of the coupling strength are $\alpha = 0.0043$ for s -wave and $\alpha = 0.0188$ for p -wave annihilation. When η takes larger value, the relic abundance is determined by the asymmetry and it is independent of α . For the same mass bound m_{\max} , asymmetric DM needs larger coupling to attain the observed value of DM relic density compared to the symmetric case. When the cross section is small, the abundance is insensitive for the increased mass. When the mass reached the maximum value, the Sommerfeld enhanced annihilation cross section is increased to satisfy the observed value of the DM relic density for different asymmetry.

Our results are important when the affect of Sommerfeld enhancement is significant at low velocity limit. The Sommerfeld effect hints notable indirect detection signals from asymmetric DM antiparticle. This allows us to examine the asymmetric DM by the Cosmic Microwave Background (CMB) observation, the Milky ways and Dwarf galaxies.

Acknowledgments

The work is supported by the National Natural Science Foundation of China (U2031204, 11765021) and Natural Science Foundation of Xinjiang Uygur Autonomous Region (2022D01C52).

References

- [1] S. Nussinov, Phys. Lett. B **165**, (1985) 55; K. Griest and D. Seckel. Nucl. Phys. B **283**, (1987) 681; R. S. Chivukula and T. P. Walker, Nucl. Phys. B **329**, (1990) 445; D. B. Kaplan, Phys. Rev. Lett. **68**, (1992) 742; D. Hooper, J. March-Russell and S. M. West, Phys. Lett. B **605**, (2005) 228 [arXiv:hep-ph/0410114]; JCAP **0901** (2009) 043 [arXiv:0811.4153v1 [hep-ph]]; H. An, S. L. Chen, R. N. Mohapatra and Y. Zhang, JHEP **1003**, (2010) 124 [arXiv:0911.4463 [hep-ph]]; T. Cohen and K. M. Zurek, Phys. Rev. Lett. **104**, (2010) 101301 [arXiv:0909.2035 [hep-ph]]. D. E. Kaplan, M. A. Luty and K. M. Zurek, Phys. Rev. D **79**, (2009) 115016 [arXiv:0901.4117 [hep-ph]]; T. Cohen, D. J. Phalen, A. Pierce and K. M. Zurek, Phys. Rev. D **82**, (2010) 056001 [arXiv:1005.1655

- [hep-ph]]; J. Shelton and K. M. Zurek, Phys. Rev. D **82**, (2010) 123512 [arXiv:1008.1997 [hep-ph]];
- [2] A. Belyaev, M. T. Frandsen, S. Sarkar and F. Sannino, Phys. Rev. D **83** (2011), 015007 doi:10.1103/PhysRevD.83.015007 [arXiv:1007.4839 [hep-ph]].
- [3] K. Petraki, L. Pearce and A. Kusenko, JCAP **07** (2014), 039 doi:10.1088/1475-7516/2014/07/039 [arXiv:1403.1077 [hep-ph]].
- [4] N. Aghanim *et al.* [Planck], Astron. Astrophys. **641** (2020), A6 [erratum: Astron. Astrophys. **652** (2021), C4] doi:10.1051/0004-6361/201833910 [arXiv:1807.06209 [astro-ph.CO]].
- [5] M. L. Graesser, I. M. Shoemaker and L. Vecchi, JHEP **1110**, (2011) 110 [arXiv:1103.2771 [hep-ph]].
- [6] H. Iminiyaz, M. Drees and X. Chen, JCAP **1107**, (2011) 003 [arXiv:1104.5548 [hep-ph]].
- [7] J. L. Feng, M. Kaplinghat, H. Tu and H. B. Yu, JCAP **07** (2009), 004 doi:10.1088/1475-7516/2009/07/004 [arXiv:0905.3039 [hep-ph]].
- [8] P. Agrawal, F. Y. Cyr-Racine, L. Randall and J. Scholtz, JCAP **1708** (2017) 021 doi:10.1088/1475-7516/2017/08/021 [arXiv:1702.05482 [astro-ph.CO]].
- [9] P. Agrawal, F. Y. Cyr-Racine, L. Randall and J. Scholtz, JCAP **05** (2017), 022 doi:10.1088/1475-7516/2017/05/022 [arXiv:1610.04611 [hep-ph]].
- [10] M. Cirelli, P. Panci, K. Petraki, F. Sala and M. Taoso, JCAP **05** (2017), 036 doi:10.1088/1475-7516/2017/05/036 [arXiv:1612.07295 [hep-ph]].
- [11] A. Sommerfeld, Ann. Phys. **403** (1931) 257-330
- [12] J. Hisano, S. Matsumoto and M. M. Nojiri, Phys. Rev. D **67** (2003), 075014 doi:10.1103/PhysRevD.67.075014 [arXiv:hep-ph/0212022 [hep-ph]].
- [13] J. Hisano, S. Matsumoto and M. M. Nojiri, Phys. Rev. Lett. **92** (2004), 031303 doi:10.1103/PhysRevLett.92.031303 [arXiv:hep-ph/0307216 [hep-ph]].
- [14] B. von Harling and K. Petraki, JCAP **12** (2014), 033 doi:10.1088/1475-7516/2014/12/033 [arXiv:1407.7874 [hep-ph]].
- [15] M. Pospelov and A. Ritz, Phys. Lett. B **671** (2009), 391-397 doi:10.1016/j.physletb.2008.12.012 [arXiv:0810.1502 [hep-ph]].
- [16] J. D. March-Russell and S. M. West, Phys. Lett. B **676** (2009), 133-139 doi:10.1016/j.physletb.2009.04.010 [arXiv:0812.0559 [astro-ph]].
- [17] K. Petraki, M. Postma and J. de Vries, JHEP **04** (2017), 077 doi:10.1007/JHEP04(2017)077 [arXiv:1611.01394 [hep-ph]].

- [18] J. Hisano, S. Matsumoto, M. M. Nojiri and O. Saito, Phys. Rev. D **71** (2005), 063528 doi:10.1103/PhysRevD.71.063528 [arXiv:hep-ph/0412403 [hep-ph]].
- [19] N. Arkani-Hamed, D. P. Finkbeiner, T. R. Slatyer and N. Weiner, Phys. Rev. D **79** (2009), 015014 doi:10.1103/PhysRevD.79.015014 [arXiv:0810.0713 [hep-ph]].
- [20] H. An, M. B. Wise and Y. Zhang, Phys. Rev. D **93** (2016) no.11, 115020 doi:10.1103/PhysRevD.93.115020 [arXiv:1604.01776 [hep-ph]].
- [21] H. An, M. B. Wise and Y. Zhang, Phys. Lett. B **773** (2017), 121-124 doi:10.1016/j.physletb.2017.08.010 [arXiv:1606.02305 [hep-ph]].
- [22] T. Bringmann, F. Kahlhoefer, K. Schmidt-Hoberg and P. Walia, Phys. Rev. Lett. **118** (2017) no.14, 141802 doi:10.1103/PhysRevLett.118.141802 [arXiv:1612.00845 [hep-ph]].
- [23] I. Baldes and K. Petraki, JCAP **09** (2017), 028 doi:10.1088/1475-7516/2017/09/028 [arXiv:1703.00478 [hep-ph]].
- [24] A. Abudurusuli and H. Iminniyaz, [arXiv:2001.08404 [hep-ph]].
- [25] A. Sulitan, H. Iminniyaz and M. Baoxia, Chin. J. Phys. **70** (2021), 117-124 doi:10.1016/j.cjph.2020.12.015 [arXiv:2009.13410 [hep-ph]].
- [26] A. Kamada, H. J. Kim and T. Kuwahara, JHEP **12** (2020), 202 doi:10.1007/JHEP12(2020)202 [arXiv:2007.15522 [hep-ph]].
- [27] M. Duerr, K. Schmidt-Hoberg and S. Wild, JCAP **09** (2018), 033 doi:10.1088/1475-7516/2018/09/033 [arXiv:1804.10385 [hep-ph]].
- [28] J. L. Feng, M. Kaplinghat and H. B. Yu, Phys. Rev. D **82** (2010) 083525 doi:10.1103/PhysRevD.82.083525 [arXiv:1005.4678 [hep-ph]].
- [29] S. Cassel, J. Phys. G **37** (2010), 105009 doi:10.1088/0954-3899/37/10/105009 [arXiv:0903.5307 [hep-ph]].
- [30] R. J. Scherrer and M. S. Turner, Phys. Rev. D **33**, (1986) 1585, Erratum-ibid. D **34**, (1986) 3263.